Synthesis of Silver Nanoparticles Reduced by Bingol Propolis and Evaluation of Antioxidant, Cytotoxic and Anticancer Activities in PC-3 Cells

Gökhan Dervişoğlu
Ekrem Darendelioğlu
Gürkan Aykutoğlu
Adnan Ayna
BÜLENT KAYA (b_kaya_tr@yahoo.com)
Bingöl Üniversitesi https://orcid.org/0000-0002-1216-6441

Research Article

Keywords: Antioxidant Activity, Cytochrome C, PC-3, Pro-Caspase-3, Immunoblotting.

Posted Date: March 18th, 2022

DOI: https://doi.org/10.21203/rs.3.rs-1454565/v1

Abstract

Green synthesis of silver nanoparticles (AgNPs) has been reported in several studies. However, no study focused on synthesis, characterization, and investigation of anticancer and antioxidant activities of AgNPs using Bingöl propolis. The morphology and physical properties of PrAgNPs (propolis-AgNPs) were characterized by UV-Vis spectrum of the characteristic silver surface plasmon resonance band, FTIR, XRD, SEM, zeta potential and DLS analysis. XRD and zeta potential analysis revealed a potential of-24.6 mV and formation of cubic crystals, with an average size of 3.45 nm, and a wide band at 420 nm was detected in UV-vis spectroscopy. The *in vitro* antioxidant capacities of PrAgNPs were evaluated by DPPH radical scavenging, metal chelating, and hydroxyl radical scavenging activities. The cytotoxicity and anticancer activities of ethanolic extract of propolis (EEP) and PrAgNPs were investigated on PC-3 cell lines by WST-1 assay and western blotting. The results demonstrated that PrAgNPs showed higher antioxidant activity than the EEP. The synthesized PrAgNPs were also shown to inhibit PC-3 cell proliferation. In the immunoblotting study, the expression of levels of apoptotic markers pro-caspase-3 and cytochrome c confirmed apoptosis induced by PrAgNPs. The current study reveals that green synthesized PrAgNPs possess antioxidant, anticancer, and apoptotic activities on human prostate cancer cell line PC-3 and pave the way for the possible treatment of the various cancers.

1. Introduction

Nanotechnology is the science that deals with the synthesis of particles between 1-100 nm. Physical production, bottom-up production synthesis and top-down synthesis method were used as chemical methods for the synthesis of nanoparticles with nanotechnology. However, these methods have high costs, cause environmental pollution and release of toxic agent. The easy, inexpensive, environmentally friendly biological green synthesis method has emerged as a synthesis route with increasing interest in recent year [1–3]. In this approach, natural compounds from microorganisms such as algae, bacteria, fungi, or plants are used as precursors to reduce metal ions [4–6]. The green synthesis of NPs is a simple, cheap, and environmentally friendly route as it uses nontoxic solvents like water. NPs in particular have shown broad-spectrum antibacterial, antioxidant, anticancer activities along with their use in drug delivery systems [7–14].

Propolis, also known as bee glue, is produced by honeybees for constructing and maintaining the hives. Until recently, several independent research groups have comprehensively studied its various biological activities and health benefits [15–18]. The projected benefits of propolis on health are comprehensively explored by revealing its antimicrobial [19], wound healing [20], cardiovascular protecting [21], and maintenance of neural functionality [22].. These activities of propolis are attributed to its rich bioactive phytochemical contents. Some of the important bioactive components of propolis contain phenolics, flavonoids, amino acids, esters, fatty acids, lignans, minerals, alcohols, and vitamins [23–25]. The amount and type of these constituents differ based on the climate, plant type, and production location.

The machinery by which propolis maintains health seems to be primarily associated with its anti-oxidant and anti-inflammatory properties, even though the scope and range of its biological impacts are wide-ranging in most circumstances. Several studies about the anti-cancer and antioxidant activities of propolis have been deposited in the literature. İndependent research groups reported the cytotoxic and anti-proliferative influences of propolis and its NPs on various cancer cell lines [26–30]. However, there is no such study examining synthesis, characterization, and investigation of anticancer and antioxidant activities of AgNPs using Bingöl propolis (PrAgNPs). In the current study, we report the biosynthesis of Bingöl propolis mediated silver nanoparticles for the first time. The physicochemical parameters of the PrAgNPs were evaluated by several analytical techniques as the size, shape, and stability of the nanoparticles greatly affect their biological activities. The *in vitro* biological activities (antioxidant, cytotoxic and anticancer) PrAgNPs were also analysed against PC-3 prostate cancer cell line within this study.

2. Materials And Methods

2.1. Materials

2.1.1. Propolis

Fresh propolis was obtained from Bingöl Province and used in this study. Propolis was purchased from local beekeepers registered with Bingöl beekeepers association.

2.1.2. Chemicals

Gallic acid, Quercetin, Folin-Ciocalteu reagent, ferrozine, trichloroacetic acid (TCA), 1.1-diphenyl-2-picrylhydrazyl (DPPH)hydrogen peroxide, 1.10-phenanthroline, α-tocopherol, sodium carbonate, sodium phosphate, sodium nitrite, sodium nitrate, sodium molybdate, ammonium molybdate, aluminum chloride, ferrous chloride, ferrous cyanide, and $AgNO_3$ were purchased from Sigma Aldrich (USA) and of analytical grade. Butylated hydroxyanisole (BHA), butylated hydroxytoluene (BHT) were procured from Merck (Darmstadt, Germany) and of analytical grade. RPMI 1640 medium, penicillin-streptomycin solution (100x), fetal bovine serum albumin, trypsin-EDTA 1x, and 1x PBS were purchased from Biological Industries (Israel). Protein markers, APS, acrylamide, TEMED, and pre-stained sodium dodecyl sulfate-polyacrylamide gel electrophoresis (SDS-PAGE) standards were obtained from Bio-Rad (Irvine, CA, USA), and an enhanced chemiluminescence (ECL) kit was purchased from Thermo Scientific (Madison, WI, USA). Protease inhibitor cocktail was purchased from Pierce Biotechnology Inc. (Rockford, IL, USA). Polyvinylidene difluoride (PVDF) membrane was bought from Millipore (Millipore, USA). Mouse monoclonal and secondary antibodies (Goat Anti-Mouse IgG) were purchased from Santa Cruz Biotechnology.

2.2 Methods

2.2.1. Preparation of ethanolic extract of propolis

The ethanolic extract of propolis (EEP) was obtained as described by Jonaidi et al. (2018) [31] with some modifications. 5 g of propolis was extracted in 50 mL ethanol (70%) with continuous stirring at 150 rpm in an orbital shaker for 24 hours at room temperature. The suspension was filtered by using Whatman filter paper (No. 3, Sigma-Aldrich). The filtrate was centrifugated at 600 x g for 20 min. The clear supernatant was then vaporized in a rotary evaporator at 40°C, and the propolis powder was obtained by freeze-drying.

2.2.2. Synthesis of Propolis AgNPs (PrAgNPs)

PrAgNPs were synthesized following a modified procedure described by Ghramh et al., 2019 [32]. Briefly, 5 mL of ethanolic extract of propolis was mixed in 95 mL 1 x 10^{-3} mM aqueous $AgNO_3$ solution and stirred at 40^{o}C temperature for 24 h. Environmentally friendly synthesis of PrAgNPs, the presence of the formation of the reaction was observed, with the reaction medium changing from light yellow to dark brown. This color change mostly occurs due to the presence of biologically active substances in the content of propolis extract and the reduction in water. The functional groups of phenolic compounds (H and OH), takes part in the bioreduction of Ag + ions to Ag(0), and hence resulting in the formation of silver nanoparticles [35]. The possible mechanism involved in this process is given in Fig. 1.

The colloidal solution of synthesized PrAgNPs was scanned in the 200–900 nm range using a UV spectrophotometer to determine the formation of PrAgNPs. The specific peak of formed AgNPs was determined at 420 nm.

2.2.3 Characterization of PrAgNPs

The bioreduction of Ag^{+} ions in solution was monitored by UV–vis spectrophotometer in the range of 200–900 nm wavelength (Shimadzu UV-3600 UV-VIS-NIR Spectrophotometer). Fourier Transforms infrared spectroscopy (FT-IR) analysis was used to identify biomolecules in the ethanolic extract of propolis responsible for biological activities and stabilization of nanoparticles. FT-IR spectra were analyzed by the dried direct method for propolis ethanolic extract powders and dried PrAgNPs using an FT-IR spectrometer (Perkin Elmer Spectrum 100) in the wavelength range of 4,000 to 400 cm^{-1}. The size distribution, stability, elemental composition and purity of PrAgNPs in solution was analyzed by DLS and particle size analyzer (ZETA Seizers Nanoseries (Malvern Instruments Nano ZS). The morphology and clustered states of PrAgNPs were analysed by scanning electron microscopy (JEOL). For analysis, drop of sample was dried on a carbon-coated copper grid and then images were taken at different magnification.

XRD characterization of the dried PrAgNPs was performed using a Rigaku Optima IV diffractometer with Cu Kα radiation for generating 2θ data (λ = 0.15406 nm) operated at 30 mA current and at 40 kV voltage. The results were compared with standard JCPDS library to determine the crystalline structure. We estimated the average crystalline size by formula of Debye–Scherrer's, $D=(0.9\lambda/\beta Cos\theta)$ where λ is the wavelength of the X-ray source, β is the angular FWHM of the XRD diffraction peak and θ is the Bragg

angle. Inter planar spacing (d) was calculated from Bragg's Law, $2dSin\theta = n\lambda$ where n is the order of diffraction pattern.

2.2.4. Determination of flavonoid, phenolic acid and phenolic amount

The total phenolic content (TPC) in EEP and PrAgNPs were determined by the Folin-Ciocalteu method [34]. Briefly, 10 mL of methanol (80%) was mixed with 250 mg of the EEP or PrAgNPs and shaken slowly. The obtained methanolic extract was filtered and 0.5 mL of the solution was mixed with 2.5 mL of the Foline-Ciocalteu's reagent (1:10 diluted with distilled water) and 2 mL of 7.5% sodium carbonate solution in a tube test and shaken. The mixture was maintained at 45°C in a hot water bath for 15 min. The total phenolic amount (TPA) in the EEP and PrAgNPs was determined spectrophotometrically at 765 nm.Quantification was performed based on the standard curve in micrograms of gallic acid (GAE) equivalents per gram. The total phenolic acid amount (TPA) in the EEP and PrAgNPs was de-termined spectrophotometrically as described in [35–37]. The results were given according to sinapic acid standard and expressed as micrograms of sinapic acid equivalents (SAE) per gram.

Flavonoid amounts (TFC) of the EEP and PrAgNPs were calculated spectrophotometrically using the aluminum chloride method as previously described by Barros et al. (2007)[38]. Briefly, 150 µL of 15% $NaNO_2$ solution and 1 mL distilled water were added to each of those of 250 µL of EEP and 250 µL of PrAgNPs samples, then vortexed and incubated for 6 minutes in dark at the 25°C. After that, these mixtures were mixed with 75 µL of 10% $AlCl_3$ solution, vortexed, and incubated for 5 minutes in dark at the 25°C. After incubation, 1 mL of 4% NaOH solution and 2.5 mL distilled water were added, vortexed, and read immediately absorbance at 510 nm by using a spectrophotometer. The results were given according to quercetin standard and expressed as micrograms of quercetin equivalents per gram. All experiments were performed in triplicate.

2.2.5. Antioxidant activity assays

DPPH radical scavenging activities of EEP and PrAgNPs were determined using spectrophoto-metric methods described by Hatano et al. (1989) [39]. According to this method, 200 µL of $6x10^{-5}$ mol/ dm^3 DPPH solution (dissolved in ethanol) was added to each of those of 50 µL of 200 µg/mL EEP and 50 µL of 200 µg/mL PrAgNPs samples, then the mixtures were shaken vigor-ously and kept in the dark area for 60 minutes. The decolorization of the DPPH was determined by spectrophotometric absorbance at 517 nm.

DPPH scavenging activity was calculated as percent removal using the following formula.

$$\% \text{ Scavenging rate} = ((A_{Control} - A_{Sample})/A_{Control}) \times 100$$

Where $A_{Control}$, the absorbance of DPPH and A_{Sample}, absorbance measured by DPPH removal in the presence of EEP and PrAgNPs .AControl is the absorbance of the control or the blind, and ASample is the absorbance measured in the EEP and PrAgNPs [39].

Metal chelating ability was determined using the iron binding ability of EEP and PrAgNPs [43]. Briefly, 1.6 mL of deionized water and 50 µL of $2x10^{-3}$ mol/dm^3 $FeCl_2$ were added, 500 µL of each EEP and PrAgNPs. At the end of the next 30 seconds, 100 µL of $5x10^{-3}$ mol/dm^3 Ferrozine was added to this mixture. Ferrozine becomes water-soluble when it reacts with bivalent iron. The Fe^{+2}-Ferrozine complex was incubated at 25°C for 10 minutes. Immediately after incubation, absorbance was measured at 562 nm. The chelating ability of honey extract on iron is given as EDTA conjugate equivalent [40].

Hydrogen peroxide removal activities for PrAgNPs and EEP were determined using Ruch's (1989) [41] method. To determine this activity, a phosphate buffer with pH 7.4 and 43x 10 – 3 mm hydrogen peroxide were prepared fresh. EEP and PrAgNPs in the concentrations of 20 µg / mL were transferred to 1 mL of both separately tubes. Following each tube has 2.4 mL of buffer solution and finally 0.6 mL of hydrogen peroxide (43 mm). The final volume of a tube was completed to 4 mL. Both solutions were incubated at room temperature for 10 minutes and the decrease in the amount of hydrogen peroxide was recorded as a reduced absorbance in 230 nm. A buffer solution containing hydrogen peroxide was used as control (RUCH et al. 1989). The hydrogen peroxide removal was calculated as % of the following formula. [41].

$$\%\text{Inhibition rate} = (A_{Control} - A_{Sample})/A_{Control}) \times 100$$

$A_{Control}$ The absorbance of control (H_2O_2), A_{Sample} is absorbance for EEP and / or PrAgNPs.

2.2.6. Cell culture

Prostate cancer (PC-3) cells line were obtained from the American Type Culture Collection (CRL-1435, ATCC, Manassas, VA) and cultured in RPMI 1640 medium supplemented with 10% heat-inactivated fetal bovine serum (FBS) and 1% penicillin-streptomycin solution at 37°C in a humidified atmosphere with 5% CO_2.

2.2.6.1 Cell Viability Assay

The effects of EEP and PrAgNPs at concentrations between 15.625–250 µg/mL on the viability of PC-3 cells were evaluated as described in our previously published article [40] using the WST-1 cell proliferation assay kit (Clontech, USA). 15×10^3 PC-3 cells/mL were treated as given in cell culture and treatment. Subsequent to that, 5 µl of WST-1 was added into each well of 96-well plate. Then, the suspension was incubated for 120 min and the absorbances were measured at a wavelength of 450 nm (reference: 630 nm).

2.2.6.2. Western Blotting Analysis

The protein samples were separated on 12% polyacrylamide gel (Clear page precast gel, C.B.S. Scientific, CA). These proteins were blotted onto nitrocellulose membrane (0.2 µm) with Trans-Blot Turbo Transfer System (Bio-Rad, USA). for one h. Subsequently, the surfaces of the nitrocellulose membranes were blocked in the presence of 5% (w/v) BSA in TBS-Tween 20 (0.05% TBS-T) for one h. these Nitrocellulose membranes, cytochrome c (1000-fold dilution, sc-13156, mouse monoclonal, Santa Cruz Biotechnology),

caspase-3 (500-fold dilution, sc- 271759, mouse monoclonal, Santa Cruz Biotechnology) were used as primary antibodies. In addition, GAPDH (500-fold dilution, sc-365062, mouse monoclonal, Santa Cruz Biotechnology) antibodies were preferred to correct for loading and transfer changes between samples. Concisely, afterward five washing for 3 min in TBS-T, secondary antibodies were utilized for incubation during 1.5 h at 37 ^{o}C. After washing five times at regular time intervals for 3 min in TBS-T, bound antibodies were signaled by ECL (Advansta, CA). Density amounts of proteins were calculated using GelDoc EZ and Image Lab 5.2.1 software (Bio-Rad, USA). The relative protein expressions intensity of the samples was normalized by the intensity of reference protein (GAPDH) expression. The intensity of the target protein band/reference (GAPDH) was calculated by formulating the intensity of the protein band with the expression.

2.7. Statistical Analysis

All the data were means of three replicates. One-way analysis of variance (ANOVA) in different concentrations of the propolis extract and the extract with AgNPs were analyzed via SPSS (version 17). Differences with $p \leq 0.05$ were considered as statistically significant. ANOVA has been performed through Statistics 8.1 software. All pairwise comparison of means was performed with Tukey's Honest Significant Difference (antioxidant tests) and Student t test (vitality test and western blot). Standards that differed at $p \leq 0.05$ were considered to be statistically significant.

3. Result And Discussion

3.1. Characterization of silver nanoparticles

3.1.1. UV–visible spectroscopic analysis

The formation of PrAgNPs was examined and confirmed via UV-vis spectroscopy to evaluate the signature surface plasmon resonance (SPR) bands. It was previously reported that the SPR occurs at 420 nm, revealing that nucleation of AgNPs initiates with the start of the reaction, and the size remains unchanged throughout the reaction [8]. The UV–Vis absorption analysis revealed the sharp absorbance at around 450 nm (Fig. 2-430 nm), which was specific for AgNPs. A single SPR band indicates the formation ıf spherical nanoparticles, while presence of two or more SPR bands indicates formation of anisotropic molecules. In our study an additional peak for PrAgNPs was observed at 260 nm (Fig. 2). Holubnycha et al. (2018) reported that AgNPs gave a rise at 264 nm, and this peak was taken at the beginning of the formation of AgNPs via the reduction of Ag + ions to Ag0 [42]. This peak was probably formed due to the presence of polyphenolic compounds that promote the reduction of silver ions.

3.1.2. SEM analysis

SEM investigated the morphological, structural, and size of AgNPs. From the SEM image, it could be concluded that larger particles of AgNPs have been shaped owing to the aggregation of nanoparticles probably induced by the evaporation of the solvent and long incubation period (Fig. 3).

3.1.3 XRD analysis

Figure 4 demonstrated XRD analysis of PrAgNPs illustrating four characteristic diffraction peaks at 2θ = 37.9°, 44.31°, 64.45°, 77.16°, 80.99 that could be indexed to (111), (200), (220), (311) and (222) peaks representing characteristic diffraction of elemental metal Ag^0 confirming the formation of cubic crystalline AgNPs (JCPDS card No.04-0784) [43, 44].

Average particle size was calculated using Debye Scherrer equation: D = 0.9λ/βcosθ where D is the size of the crystal (Nanoparticle crystal formed), λ is the wavelength of the X-ray (Cu:1.5406 A°), β is FWHM, the maximum of the diffraction peak, and θ the Bragg (2 theta) angle. The average particle size was calculated as 3.45 nm using the Debye Scherrer equation in Table 1.

Table 1
Nanoparticle Size Calculation of XRD Pattern

Peak Position (2 Theta)	FWHM	D spacing (nm)	Average of D spacing (nm)
37,9	1,45778	3,921982	3,453726
44,31	4,99852	4,401589	
64,45	6,36134	1,474674	
77,16	2,3088	1,708433	
80,99	2,66365	5,761953	

3.1.4. DLS and Zeta potential analysis

Figure 4a, b illustrates the DLS and Zeta size distribution by intensity image of PrAgNPs. It was observed that the size distribution of PrAgNPs varied from 7.84 to 265.60 nm, and the mean of PrAgNPs' particle size distribution was determined as 66.17- 132.34 nm (Fig. 5a).. It was observed that the data obtained from DLS and Zeta size distribution confirmed each other. The zeta potential of PrAgNPs was also investigated (Fig. 5c). The zeta potential of PrAgNPs showed a sharp peak at − 24.6 ± 7.1mV at pH close to 7 (Fig. 5c). It could be concluded that the surface of the PrAgNPs was loaded with the negative charge, the negative value confirmed the electrostatic repulsion among the particles, and the particles were pretty stable.

3.1.5. FT-IR analysis of PrAgNPs

FT-IR analysis was performed to determine that these biomolecules are thus a capping agent, function and form Ag-nanoparticles from Ag ions and form the PrAgNPs stack (Fig. 6). Ramadan et al. (2012) [45] have shown that phytochemical analysis of propolis ethanolic extract contains flavonoids, carbohydrates &/or glycosides, sterols, and terpenes not contain volatiles, coumarins, alkaloids &/or nitrogenous

compounds, tannins, or saponins. The different spectrums of IR bands have been described in our previous study as aliphatic amines (1040–1053 cm^{-1}), the carboxylic acid (1050–1300 cm^{-1}), amine-amide (1180–1360 cm^{-1}), aromatic amines (1300–1370 cm^{-1}), alkanes (1340–1470 cm^{-1}), C = C aromatic ring (1500–1600 cm^{-1}), C = C alkenes (1610–1680 cm^{-1}), carbonyl (1690–1760 cm^{-1}), alkyne (2100–2260 cm^{-1}), alkanes C-H (2850–2970 cm^{-1}), alcohol, and hydroxyl (3200–3650 cm^{-1}), [35]. In propolis ethanolic extract (EEP) (Fig. 6a), the peaks were obtained at 660, 685, 692, and 700 (C-Cl_4 and C-H aromatics), 750 and 795 (C-Cl_4), 999 (C-H aromatics), 1176, 1225, and 1230 (carboxylic acid), 1525 (C = C aromatic ring), 1625 (C = C alkenes), 1700 (carbonyl), 2916.66 (alkanes), and 3325.39 (-OH) cm^{-1}, respectively. Similarly, in PrAgNPs (Fig. 6b), the peaks were observed at 685 (C-Cl_4 and C-H aromatics), 750 and 795 (C-Cl_4), 1176, 1225, and 1230 (carboxylic acid), 1385 (alkanes), 1525 (C = C aromatic ring), 1625 (C = C alkenes), 1700 (carbonyl), 2916.66 (alkanes), and 3325.39 (-OH) cm^{-1}, respectively. It was seen that the IR bands of EEP and PrAgNPs intersect at the values of 685, 750, 795, 1176, 1225, 1230, 1525, 1625, 1700, 2916.66, and 3325.39 cm^{-1}. The results showed that PrAgNPs were synthesized from silver nitrate and propolis ethanolic extract.

3.2. Total phenolic, phenolic acid and total flavonoid contents

It is generally known that the polyphenolic content gives a clue about its antioxidant potential/activity. In this study, the amounts of polyphenolic ingredients ethanolic extract of propolis and PrAgNPs were assessed, determining total phenolic (TPC), phenolic acid (TPA), and flavonoid contents (TFC). Total phenolic, phenolic acid, and flavonoid content amounts of ethanolic extract of propolis and PrAgNPs were given in Table 2. The TPC, TPA, and TFC of the PrAgNPs were found as approximately 1/2, 1/3, and 1/3 of propolis ethanolic extract, respectively. The decrease in the TPC, TPA, and TFC of the PrAgNPs, seen in Table 1, can be explained with the AgNPs preferentially adsorb polyphenolic compounds present in the propolis ethanolic extract. Also, it was seen that these obtained data were compatible with the study by Corciovă et al. (2019)[46].

Table 2
Phenolic, phenolic acid, and flavonoid amounts of ethanolic extract of propolis (EEP) and PrAgNPs

Samples	Phenolic Amounts (µg GAE/g d.w.)	Phenolic Acid Amounts (µg SAE/g d.w.)	Flavonoid Amounts (µg QE /g d.w.)
EEP	866.34 ± 48.57	12525.00 ± 730.87	929.17 ± 410.51
PrAgNPs	474.77 ± 9.58	4150.00 ± 548.01	295.83 ± 104.10

3.3. *In vitro* antioxidant activities of EEF and PrAgNPs

In general, phenolics are known to exhibit various in *vivo/vitro* antioxidant activities. Different methods such as 1,1-diphenyl-2-picrylhydrazil (DPPH), metal chelation, and hydroxyl radical scavenging have been proposed in the literature to evaluate the antioxidant activities of EEP and PrAgNPs in order to determine theirs *in vitro* antioxidant capacity. DPPH is a free radical widely used in antioxidant activity experiments to reveal various samples' free radical scavenging ability. In the presence of an antioxidant, the DPPH reacts with the antioxidant and DPPH free radical concentration changes in the media. The DPPH method is based on the spectrophotometric measurement of these DPPH free radical concentration changes [547 – 51]. DPPH free radical scavenging activities of EEP and PrAgNPs at concentrations of 200 µg/mL are shown in Fig. 7A. Treatment with EEP and PrAgNPs inhibited DPPH free radical activity at the rate of 17.06% and 67.64%, respectively. It was observed that PrAgNPs had approximately three folds more DPPH free radical scavenging activity than EEP. In a different study, Corciovă et al. (2019) [46] estimated the IC_{50} values of AgNpPs and propolis extract prepared with propolis water extract as 33.65 ± 0.03 mg/mL- 0.45 ± 0.005 mg/mL, respectively. In another study, the percentage of scavenging activity of AgNP (1 mg/mL), Microchaete extract (1 mg/mL) and standard (1 mg/mL) were found as 75.62 ± 2.31%, 8.88 ± 2.60% and 95.67 ± 2.31%, respectively [49]. These results and our results indicate that the nanoparticle systems created with propolis extracts had higher DPPH radical removal than the propolis extracts. When the effect of concentrations in the studies ignored, the rates were found to be close to each other. When evaluated in terms of concentration, the ratios diluted 5 times in our study gave results close to those of other studies. This finding reveals that the efficacy of EEP and PrAgNPs in this study is higher than that of AgNPs obtained from the studies we discussed above.Metal chelating activities of EEP and PrAgNPs as another antioxidant activity ability were examined, and the results were evaluated as % rate (Fig. 7B). EEP showed at the rate of 57.23% metal-chelating activity. AgNPs supplementation increased the metal chelating activity of propolis by the rate of 19.98%, providing PrAgNPs to display at the rate of 66.95% metal chelating activity. In a different study, FRAP assay revealed that EC_1 value of Ascorbic acid, AgNPs, and *Microchaete* aqueous extract were 0.321 mg/mL, 0.523 mg/mL, and 3867.2 mg /mL, respectively [50]. In this study, EEP was found to be 8.49 ± 0.027 mg/mL and PrAgNPs 9.94 ± 0.204 mg/mL EDTA equivalent. EC1 of PrAgNPs amd EEP were calculated as 0.15 ± 0.00 mg/ mL. and 0.50 ± 0.0 mg/mL. These results are also in close agreement with the results of our study.

Hydroxyl radical scavenging activities of EEP and PrAgNPs were investigated by using Fenton reaction, and results are indicated as % inhibition of hydroxyl radical in Fig. 7C. It was determined that PrAgNPs inhibited hydroxyl radicals by 82.30%, while EEP inhibited hydroxyl radicals by 68.38%. According to these results, it is understood that PrAgNPs have approximately 20.36% more hydroxyl radical scavenging activity than EEP. In another study, the H_2O_2 scavenging activity of different propolis samples was determined to be between 35–54% [47]. Shaheen et al. (2021) [49] reported H_2O_2 radical scavenging activity of ascorbic acid, *Microchaete* extract, and AgNPs as 63.206, 1.976, and 53.120, respectively. When the results of our study were compared with these studies, higher H_2O_2 radical scavenging activities were obtained. The reason for obtaining higher antioxidatin activities in our study could be atribbuted to the the smaller nanoparticle size and the difference in the propolis content. With the

increase in the number of nanoparticles per unit volume in small sizes, higher antioxidant values were achieved with the rise in the surface area and the rise in the number of phenolic substances transported.

The obtained values from DPPH radical scavenging, metal chelating, and hydroxyl radical scavenging activity, as shown in Fig. 7A-C, illustrate that PrAgNPs showed higher antioxidant activity than the ethanolic extract of propolis (EEP). This situation can be explained by the existence of silver that can easily donate electrons and the higher content of biomolecules having antioxidant activity at the surface of PrAgNPs, as stated in the study of Corciovă et al. (2019) [46].

3.4. Effects of EEP and PrAgNPs on PC-3 cell viability

Cytotoxic effects of the EEP and synthesized PrAgNPs were evaluated on PC-3 cells using the WST-1 assay. Figure 8 demonstrates the concentration-dependent curve from which the half-maximal (IC_{50}) cytotoxic impacts of EEP and PrAgNPs were measured. The results of our study demonstrated that, PrAgNPs showed cytotoxic effects in a concentration-dependent manner indicating is potential to be used as anticancer agents, however no such cytotoxicity has been observed for EEP treatment at low concentrations (only 125 µg/mL treatment showed cytotoxicity) IC_{50} of the PrAgNPs and EEP against PC-3 cells were 24.2 ± 08 µg/mL and 106.0 ± 28.7 µg/mL respectively. There are studies on the cytotoxic activities of propolis ethanolic extract (EEP) in some human cancer cell lines. Turan et al. (2015)[55] demonstrated that EEP exhibited strong antiproliferative effects against prostate adenocarcinoma (PC-3), hepatocellular carcinoma (HepG2), colon adenocarcinoma (WiDr), cervix adenocarcinoma (HeLa), and mammary adenocarcinoma (MCF-7) human cancer cell lines at different IC_{50} values ranging from 20.7 ± 1.3 to 62.2 ± 2.2 µg/mL. A study by Szliszka et al. (2011)[56] reported that ethanolic extract of propolis showed concentration-dependent cytotoxic effects on prostate cancer cells by inducing apoptosis. Similarly, in a recent study by Abdo et al. (2019) [57], the cytotoxic effect of propolis and propolis nanoparticles on ehrlich as cites carcinoma cells has been shown.

3.5. Effects of PrAgNPs on apoptosis linked protein levels

One of the apoptosis pathways in the mitochondrial pathway is categorized by cytochrome c levels released into the cytoplasm and reaching high levels, leading the cell to apoptosis. The increased amount of cytochrome c triggers the formation of apoptosomes, which subsequently triggers stimulation of active caspase-9 production and results in increased caspase-9 production. Activated caspase-9 then converts procaspase-3 into active caspase-3 enzyme by cleaving cellular structures, causing changes in the cell's structural morphological and biochemical properties, which will trigger apoptosis. [58–62]. We hypothesized that the prepared PrAgNPs would augment the expression of cytochrome *c* and procaspase-3 proteins in PC-3 cells. The induction of apoptosis in the PC-3 cells subjected to the synthesized PrAgNPs was studied through western blotting assay, as shown in Fig.9. The results showed that the prepared PrAgNPs and EEPs significantly increased protein levels of cytochrome *c* and procaspase-3. In another study, silver nanoparticles using *Dimocarpus Longan Lour.* Peel aqueous extract was synthesized, and its cytotoxicity effect was studied on human prostate cancer PC-3 cells. The expressions of phosphorylated BCL-2, caspase-3, stat 3, and survivin were examined by Western blot

analysis revealing its anticancer effect. The AgNPs showed concentration-dependent cytotoxicity against PC-3 cells through a decrease of stat 3, BCL-2, and surviving and an increase in caspase-3 protein levels. These results could confirm the potential anticancer application of AgNPs for prostate cancer therapy. Nonetheless, more research should be performed on the comprehensive study of molecular mechanisms and in vivo effects on prostate cancer [63]. In another study, researchers synthesized AgNPs using *Lavandula angustifolia* extract (La-AgNPs) and investigated their antiproliferative and apoptotic effects in the U87MG glioblastoma cancer cell line. The expression of apoptotic proteins caspase-3 and p53 were analyzed by western blotting. The results show that La-AgNPs induce cell death by cellular autolysis in the U87MG cell line by activating the intrinsic apoptotic pathway through p53 gene products. [64]. In one of the previous studies, Au nanoparticles were synthesized by the biogenic method from *Scutellaria barbata*-Au nanoparticles were evaluated for anticancer activity in the pancreatic cancer cell line (PANC-1). It has been reported that these nanoparticles show an adequate level of anticancer activity in pancreatic cancer cell lines (PANC-1). The synthesized Au nanoparticles lead the cell to apoptosis by decreasing Bcl-2, which has anti-apoptotic properties while increasing the level of Bax protein, which reveals the apoptotic feature in the apoptotic pathway at the protein level [65,66].

4. Conclusion

The aim of the current study was biosynthesis of Bingöl propolis silver nanoparticles using an environmentally friendly and cheap approach and evaluating its antioxidant and anticancer activities. The formation of PrAgNPs was predominantly confirmed by the UV-Vis spectrum of the characteristic silver surface plasmon resonance band, zeta sizer, X-Ray Diffraction (XRD), Scanning Electron Microscopy (SEM), and Fourier Transforms infrared spectroscopy (FT-IR) analysis. The *in vitro* antioxidant capacities of EEP and PrAgNPs were evaluated by DPPH radical scavenging, metal chelating, and hydroxyl radical scavenging activity revealing that PrAgNPs showed better antioxidant activity than the ethanolic extract of propolis (EEP). The anticancer activities of EEP and PrAgNPs were investigated on PC-3 cell lines. The synthesized PrAgNPs inhibited PC-3 cell proliferation. The apoptotic pathway activation was accompanied by increased protein expression levels of pro-caspase-3 and cytochrome c. The current research reveals that green synthesized PrgNPs have an antioxidant, anticancer, and apoptotic agent on human prostate cancer.

Abbreviations

AgNPs
Silver nanoparticles
EEP
Ethanolic Extracts of Propolis
PrAgNPs
Propolis Silver Nanoparticles System
FTIR

Fourier Transform Infrared Spectroscopy
SEM
Scanning Electron Microscopy
UV–Vis
Ultraviolet–Visible spectroscopy
XRD
X-ray Diffraction
PC-3
Human Prostate Cancer Cell Line
ATTC
American Type Culture Collection
WST-1
Cell Viability Assay Kits
BSA
Bovine Serum Albumin

Declarations

Acknowledgment

We would like to thank the Biorender program provider for the free option we used for graphic abstract and Fig. 1 drawing.

References

[1]. Khan, I., Saeed, K., & Khan, I., Nanoparticles: Properties, applications, and toxicities. Arab. J. Chem. 12(7), 908-931(2019). https://doi.org/10.1016/j.arabjc.2017.05.011.

[2]. Baig, N., Kammakakam, I., & Falath, W., Nanomaterials: a review of synthesis methods, properties, recent progress, and challenges. **Mater. Adv.** 2(6), 1821-1871(2021). https://doi.org/10.1039/D0MA00807A.

[3]. Dikshit, P. K., Kumar, J., Das, A. K., Sadhu, S., Sharma, S., Singh, S., ... & Kim, B. S., Green Synthesis of Metallic Nanoparticles: Applications and Limitations. Catalysts. 11(8), 902(2021). https://doi.org/10.3390/catal11080902.

[4]. Kim, J. S., Kuk, E., Yu, K. N., Kim, J. H., Park, S. J., Lee, H. J., ... & Cho, M. H., Antimicrobial effects of silver nanoparticles. Nanomed: Nanotechnol. Biol. Med. 3(1), 95-101(2007). https://doi.org/10.1016/j.nano.2006.12.001.

[5]. Singh R, Wagh P, Wadhwani S, Gaidhani S, Kumbhar A, Bellare J, Chopade BA., Synthesis, optimization, and characterization of silver nanoparticles from Acinetobacter calcoaceticus and their

enhanced antibacterial activity when combined with antibiotics. Int. J. Nanomedicine. 8(1), 4277-4290(2013). https://doi.org/10.2147/IJN.S48913.

[6]. Maity, G. N., Maity, P., Choudhuri, I., Sahoo, G. C., Maity, N., Ghosh, K., ... & Mondal, S., Green syn thesis, characterization, the antimicrobial and cytotoxic effect of silver nanoparticles using arabinoxylan isolated from Kalmegh. Int. J. Biol. Macromol. 162, 1025-1034(2020). https://doi.org/10.1016/j.ijbiomac.2020.06.215.

[7]. Gomathi, A. C., Rajarathinam, S. X., Sadiq, A. M., & Rajeshkumar, S., Anticancer activity of silver nanoparticles synthesized using aqueous fruit shell extract of Tamarindus indica on MCF-7 human breast cancer cell line. J Drug Deliv Sci Technol. 55, 101376(2020).https://doi.org/10.1016/j.jddst.2019.101376.

[8]. Ratan, Z. A., Haidere, M. F., Nurunnabi, M., Shahriar, S. M., Ahammad, A. J., Shim, Y. Y., ... & Cho, J. Y., Green chemistry synthesis of silver nanoparticles and their potential anticancer effects. Cancers. 12(4), 855(2020). https://doi.org/10.3390/cancers12040855.

[9]. Bedlovičová, Z., Strapáč, I., Baláž, M., & Salayová, A., A brief overview on antioxidant activity determination of silver nanoparticles. Molecules. 25(14), 3191(2020). https://doi.org/10.3390/molecules25143191.

[10]. Yousaf, H., Mehmood, A., Ahmad, K. S., & Raffi, M., Green synthesis of silver nanoparticles and their applications as an alternative antibacterial and antioxidant agents. Mater. Sci. Eng. C. 112, 110901(2020). https://doi.org/10.1016/j.msec.2020.110901.

[11]. Rajput, S., Kumar, D., & Agrawal, V., Green synthesis of silver nanoparticles using Indian Belladonna extract and their potential antioxidant, anti-inflammatory, anticancer and larvicidal activities. Plant Cell Rep. 39(7), 921-939(2020). https://doi.org/10.1007/s00299-020-02539-7.

[12]. Xu, L., Wang, Y. Y., Huang, J., Chen, C. Y., Wang, Z. X., & Xie, H., Silver nanoparticles: Synthesis, medical applications, and biosafety. Theranostics. 108996, (2020). https://doi.org/10.7150/thno.45413.

[13]. Yaqoob, A. A., Umar, K., & Ibrahim, M. N. M., Silver nanoparticles: various methods of synthesis, size affecting factors and their potential applications-a review. Appl. Nanosci. 10(5), 1369-1378(2020). https://doi.org/10.1007/s13204-020-01318-w.

[14]. Li, G., He, D., Qian, Y., Guan, B., Gao, S., Cui, Y., Wang, L., Fungus-mediated green synthesis of silver nanoparticles using *Aspergillus terreus*. Appl. Nanosci. 13(1), 466-476(2012). https://doi.org/10.3390/ijms13010466.

[15]. Ahmed, R. H., & Mustafa, D. E., Green synthesis of silver nanoparticles mediated by traditionally used medicinal plants in Sudan. Int. Nano Lett. 10(1), 1-14. (2020). https://doi.org/10.1007/s40089-019-00291-9.

[16]. Garibo, D., Borbón-Nuñez, H. A., de León, J. N. D., Mendoza, E. G., Estrada, I., Toledano-Magaña, Y., & Susarrey-Arce, A., Green synthesis of silver nanoparticles using *Lysiloma acapulcensis* exhibit high-antimicrobial activity. Sci. Rep. 10(1), 1-11(2020). https://doi.org/10.1038/s41598-020-69606-7.

[17]. Przybyłek, I., & Karpiński, T. M., Antibacterial properties of propolis. Molecules. 24(11), 2047(2019). https://doi.org/10.3390/molecules24112047.

[18]. Shehata, M. G., Ahmad, F. T., Badr, A. N., Masry, S. H., & El-Sohaimy, S. A., Chemical analysis, antioxidant, cytotoxic and antimicrobial properties of propolis from different geographic regions. Ann. Agric. Sci. 65(2), 209-217(2020). https://doi.org/10.1016/j.aoas.2020.12.001.

[19]. Refaat, H., Mady, F. M., Sarhan, H. A., Rateb, H. S., & Alaaeldin, E., Optimization and evaluation of propolis liposomes as a promising therapeutic approach for COVID-19. Int. J. Pharm. 592, 120028(2021). https://doi.org/10.1016/j.ijpharm.2020.120028.

[20]. Ripari, N., Sartori, A. A., da Silva Honorio, M., Conte, F. L., Tasca, K. I., Santiago, K. B., & Sforcin, J. M. Propolis antiviral and immunomodulatory activity: a review and perspectives for COVID-19 treatment. J. Pharm. Pharmacol. 73(3), 281-299(2021). https://doi.org/10.1093/jpp/rgaa067.

[21]. Hernandez Zarate, M. S., Abraham Juarez, M. D. R., Ceron Garcia, A., Ozuna Lopez, C., Gutierrez Chavez, A. J., Segoviano Garfias, J. D. J. N., & Avila Ramos, F., Flavonoids, phenolic content, and antioxidant activity of propolis from various areas of Guanajuato, Mexico. Food Sci. Technol. 38, 210-215(2018). https://doi.org/10.1590/fst.29916.

[22]. Anjum, S. I., Ullah, A., Khan, K. A., Attaullah, M., Khan, H., Ali, H., ... & Dash, C. K., Composition and functional properties of propolis (bee glue): A review. Saudi J. Biol. Sci. 26(7), 1695-1703(2019). https://doi.org/10.1016/j.sjbs.2018.08.013.

[23]. El Menyiy, N., Bakour, M., El Ghouizi, A., El Guendouz, S., & Lyoussi, B., Influence of Geographic Origin and Plant Source on Physicochemical Properties, Mineral Content, and Antioxidant and Antibacterial Activities of Moroccan Propolis. Int. J. Food Sci. Vol. 2021, Article ID 5570224 12 pages(2021). https://doi.org/10.1155/2021/5570224.

[24]. De Vecchi E, Drago L., Attività antimicrobica della propoli: cosa c'è di nuovo? [Propolis' antimicrobial activity: what's new?]. Infez Med.15(1) 7-1,(2007). Italian. PMID: 17515670.

[25]. Oryan, A., Alemzadeh, E., & Moshiri, A., Potential role of propolis in wound healing: Biological properties and therapeutic activities. Biomed Pharmacother. 98, 469-483(2018). https://doi.org/10.1016/j.biopha.2017.12.069.

[26]. Silva, H., Francisco, R., Saraiva, A., Francisco, S., Carrascosa, C., & Raposo, A., The cardiovascular therapeutic potential of propolis-A comprehensive review. Biology. 10(1), 27(2021). https://doi.org/10.3390/biology10010027.

[27]. Balion, Z., Ramanauskienė, K., Jekabsone, A., & Majienė, D., The Role of Mitochondria in Brain Cell Protection from Ischaemia by Differently Prepared Propolis Extracts. Antioxidants. 9(12), 1262(2020). https://doi.org/10.3390/antiox9121262.

[28]. Pratsinis, H., Kletsas, D., Melliou, E., & Chinou, I., Antiproliferative activity of Greek propolis. J. Med. Food. 13(2),286-290(2010). https://doi.org/10.1089/jmf.2009.0071.

[29]. Frión-Herrera, Y., Gabbia, D., Scaffidi, M., Zagni, L., Cuesta-Rubio, O., De Martin, S., & Carrara, M., Cuban Brown Propolis Interferes in the Crosstalk between Colorectal Cancer Cells and M2 Macrophages. Nutrients. 12(7), 2040 (2020). https://doi.org/10.3390/nu12072040.

[30]. Al-Fakeh, M., Osman, S. O. M., Gassoumi, M., Rabhi, M., & Omer, M., Characterization and Antimicrobial and Anticancer Properties of Palladium Nanoparticles Biosynthesized Optimally Using Saudi Propolis. Nanomater. 11(10), 2666(2021).https://doi.org/10.3390/nano11102666.

[31]. Forma, E., & Bryś, M., Anticancer Activity of Propolis and Its Compounds. Nutrients. 13(8), 2594(2021). https://doi.org/10.3390/nu13082594.

[32]. Azarshinfam, N., Tanomand, A., Soltanzadeh, H., & Rad, F. A., Evaluation of anticancer effects of propolis extract with or without combination with layered double hydroxide nanoparticles on Bcl-2 and Bax genes expression in HT-29 cell lines. Gene Rep. 23, 101031(2021). https://doi.org/10.1016/j.genrep.2021.101031.

[33]. Jonaidi Jafari N, Kargozari M, Ranjbar R, Rostami H, Hamedi H., The effect of chitosan coating incorporated with ethanolic extract of propolis on the quality of refrigerated chicken fillet. J. Food Process. Preserv. 42(1), e13336(2018). https://doi.org/10.1111/jfpp.13336.

[34]. Ghramh HA, Khan KA, Ibrahim EH, Ansari MJ., Biogenic synthesis of silver nanoparticles using propolis extract, their characterization, and biological activities. Science of Advanced Materials 11(6) 876-83(2019). https://doi.org/10.1166/sam.2019.3571

[35]. Tarannum, N., Divya, D. and Gautam, Y., Facile green synthesis and applications of silver nanoparticles: a state-of-the-art review. RSC Advances, 934926-34948(2019). https://doi.org /10.1039/C9RA04164H

[36]. Kaya B, Darendelioğlu E, Dervişoğlu G, Tartik M., Determination of comparative biological activities of silver nanoparticles formed by biological synthesis using *Achillea vermicularis*. Pak. J. Bot. 50(4), 1423-32(2018). http://inis.iaea.org/search/search.aspx?orig_q=RN:49055188

[37]. Gámez-Meza, N., Noriega-Rodríguez, J.A., Medina-Juárez, L.A., Ortega-García, J., Cázarez-Casanova, R. and Angulo-Guerrero, O., Antioxidant activity in soybean oil of extracts from Thompson grape bagasse. J. Am. Oil Chem. Soc. 76(12) 1445-1447, (1999). https://doi.org/10.1007/s11746-999-0182-4

[38]. Niculae M, Hanganu D, Oniga I, Benedec D, Ielciu I, Giupana R, Sandru CD, Ciocârlan N, Spinu M. Phytochemical Profile and Antimicrobial Potential of Extracts Obtained from *Thymus marschallianus* Willd. Molecules. 24(17), 3101(2019). https://doi.org/10.3390/molecules24173101

[39]. Benedec D, Vlase L, Oniga I, Mot AC, Damian G, Hanganu D, Duma M, Silaghi-Dumitrescu R., Polyphenolic composition, antioxidant and antibacterial activities for two Romanian subspecies of *Achillea distans* Waldst. et Kit. ex Willd.. Molecules. 18(8), 8725-39(2013). https://doi.org/10.3390/molecules18088725

[40]. Ielciu I, Frédérich M, Hanganu D, Angenot L, Olah N-K, Ledoux A, Crișan G, Păltinean R., Flavonoid analysis and antioxidant activities of the *Bryonia alba* L. Aerial parts. Antioxidants. 8(4):108(2019). https://doi.org/10.3390/antiox8040108

[41]. Barros L, Ferreira M-J, Queirós B, Ferreira ICFR, Baptista P., Total phenols, ascorbic acid, β-carotene, and lycopene in Portuguese wild edible mushrooms and their antioxidant activities. Food Chem. 103(2), 413-9(2007). https://doi.org/10.1016/j.foodchem.2006.07.038

[42]. Hatano T, Edamatsu R, Hiramatsu M, Mori A, Fujita Y, Yasuhara T, Yoshida T, Okuda T. Effects of the interaction of tannins with co-existing substances. VI.: effects of tannins and related polyphenols on superoxide anion radical, and on 1, 1-Diphenyl-2-picrylhydrazyl radical. Chem. Pharm. Bull. 37(8) (1989) 2016-21. https://doi.org/10.1248/cpb.37.2016

[43]. Dinis, T.C.P., V.M.C. Madeira and L.M. ve Almeidam, L. M., Action of phenolic derivates (acetoaminophen, salycilate, and 5 aminosalycilate) as inhibitors of membrane lipid peroxidation and peroxyl radicals scavengers. Arch. Biochem. Biophys. 315 161 169,(1994). DOI: 10.1006/abbi.1994.1485

[44]. Ruch RJ, Cheng SJ, Klaunig JE., Prevention of cytotoxicity and inhibition of intercellular communication by antioxidant catechins isolated from Chinese green tea. Carcinogenesis. 10,1003–1008(1989). https://doi.org/10.1093/carcin/10.6.1003

[45]. Holubnycha, V., Kalinkevich, O., Ivashchenko, O. and Pogorielov, M., Antibacterial Activity of In Situ Prepared Chitosan/Silver Nanoparticles Solution Against Methicillin-Resistant Strains of Staphylococcus aureus. Nanoscale Res. Lett. 13(1) 71,(2018). https://doi.org/10.1186/s11671-018-2482-9

[46]. Meng, Yongde., A Sustainable Approach to Fabricating Ag Nanoparticles/PVA Hybrid Nanofiber and Its Catalytic Activity, Nanomaterials. 5 1124-1135, (2015). https://doi.org/10.3390/nano5021124

[47]. Kamalanathan, Ashok & Jayaprakash, P. & Kanakarajan, Sivakumari & Selvaraj, Rajesh & Durai, Prabhu & Chandrasekar, D., Anticancer Potential of Green Synthesized Silver Nanoparticles of Sargassum Wightıı Agaınts Human Prostate Cancer (PC-3) Cell Line. Eur. J. Pharm. Med. Res. 4 275-287(2017). http://hdl.handle.net/10603/259238.

[48]. Ramadan A, Soliman G, Mahmoud SS, Nofal SM, Abdel-Rahman RF., Evaluation of the safety and antioxidant activities of *Crocus sativus* and Propolis ethanolic extracts. J. Saudi Chem. Soc. 16(1), 13-21(2012). https://doi.org/10.1016/j.jscs.2010.10.012

[49]. Corciovă A, Mircea C, Burlec A-F, Cioancă O, Tuchiluş C, Fifere A, Lungoci A-L, Marangoci N, Hăncianu M., Antioxidant, Antimicrobial And Photocatalytic Activities Of Silver Nanoparticles Obtaiined By Bee Propolis Extract Assisted Biosynthesis, Farmacia 67(3) 482-9,(2019). https://doi.org/10.31925/farmacia.2019.3.16.

[50]. Nagai T, Inoue R, Inoue H, Suzuki N., Preparation and antioxidant properties of water extract of propolis, Food Chem. 80(1) 29-33,(2003). https://doi.org/10.1016/S0308-8146(02)00231-5.

[51]. Sharma, S.K. and A.P. Singh, In vitro antioxidant and free radical scavenging activity of *Nardostchys jatamansi* DC. J. Acupunct. Meridian Stud. 5(3) 112-118,(2012). https://doi.org/10.1016/j.jams.2012.03.002.

[52]. Shaheen H., Suresh K. V., Durdana Y., Hemlata, M. Moshahid A. R., Tasneem F., Facile green bio-fabricated silver nanoparticles from Microchaete infer dose-dependent antioxidant and anti-proliferative activity to mediate cellular apoptosis, Bioorg. Chem. 107104535,(2021). https://doi.org/10.1016/j.bioorg.2020.104535.

[53]. Meng, G.E. & Tian, Y & Yang, Y & Shi, J., Evaluation of DPPH free radical scavenging activity of various extracts of Ligularia fischeri in vitro: A case study of Shaanxi region. Ind. J. Pharm. Sci. 78(4), 436-42(2016). https://doi.org/10.4172/pharmaceutical-sciences.1000137.

[54]. Nna, V. U., Bakar, A. B. A., Lazin, M. R. M. L. M., & Mohamed, M., Antioxidant, anti-inflammatory, and synergistic anti-hyperglycemic effects of Malaysian propolis and metformin in streptozotocin-induced diabetic rats. Food Chem. Toxicol. 120 305-320,(2018). https://doi.org/10.1016/j.fct.2018.07.028.

[55]. Turan I, Demir S, Misir S, Kilinc K, Mentese A, Aliyazicioglu Y, Deger O., Cytotoxic effect of Turkish propolis on liver, colon, breast, cervix and prostate cancer cell lines. Trop. J. Pharm. Res. 14(5), 777-82(2015). https://doi.org/10.4314/tjpr.v14i5.5.

[56]. Szliszka E, Czuba ZP, Bronikowska J, Mertas A, Paradysz A, Krol W., Ethanolic Extract of Propolis Augments TRAIL-Induced Apoptotic Death in Prostate Cancer Cells, Evid. Based Complement. Alternat. Med. vol. 2011, Article ID 535172, 11 pages(2011). https://doi.org/10.1093/ecam/nep180.

[57]. Abdo JA, Alsharif FM, Salah N, Elkhawaga OAY., Cytotoxic Effect of Propolis Nanoparticles on Ehrlich Ascites Carcinoma Bearing Mice. Adv. Nano Res. 8(4) 55-70,(2019). https://doi.org/10.4236/anp.2019.84005.

[58]. Chipuk JE, Kuwana T, Bouchier-Hayes L, Droin NM, Newmeyer DD, Schuler M, Green DR., Direct activation of Bax by p53 mediates mitochondrial membrane permeabilization and apoptosis. Science.

303(5660), 1010-1014(2004). https://doi.org/10.1126/science.1092734.

[59]. Darendelioglu E, Aykutoglu G, Tartik M, Baydas G., Turkish propolis protects human endothelial cells in vitro from homocysteine-induced apoptosis. Acta Histochem. 118(4) 369-76,(2016). https://doi.org/10.1016/j.acthis.2016.03.007.

[60]. Izuta H, Shimazawa M, Tazawa S, Araki Y, Mishima S, Hara H., Protective effects of Chinese propolis and its component, chrysin, against neuronal cell death via inhibition of mitochondrial apoptosis pathway in SH-SY5Y cells. J. Agric. Food Chem. 56(19), 8944-53(2008). https://doi.org/10.1021/jf8014206.

[61]. Kim AD, Han X, Piao MJ, Hewage SRKM, Hyun CL, Cho SJ, Hyun JW., Esculetin induces death of human colon cancer cells via the reactive oxygen species-mediated mitochondrial apoptosis pathway. Environ. Toxicol. Pharmacol. 39(2) 982-9,(2015). https://doi.org/10.1016/j.etap.2015.03.003.

[62]. Kroemer G, Dallaporta B, Resche-Rigon M., The mitochondrial death/life regulator in apoptosis and necrosis. Annu. Rev. Physiol. 60(1) 619-42,(1998). https://doi.org/10.1146/annurev.physiol.60.1.619.

[63]. He, Y., Du, Z., Ma, S., Cheng, S., Jiang, S., Liu, Y., ... & Zheng, X., Biosynthesis, antibacterial activity and anticancer effects against prostate cancer (PC-3) cells of silver nanoparticles using *Dimocarpus longan Lour.* peel extract. Nanoscale Res. Lett. 11(1) 1-10,(2016). https://doi.org/10.1186/s11671-016-1511-9.

[64]. Simsek, A., Pehlivanoglu, S., & Acar, C. A., Anti-proliferative and apoptotic effects of green synthesized silver nanoparticles using *Lavandula angustifolia* on human glioblastoma cells. 3 Biotech. 11(8) 1-10,(2021). https://doi.org/10.1007/s13205-021-02923-4.

[65]. Wang, L., Xu, J., Yan, Y., Liu, H., Karunakaran, T., & Li, F., Green synthesis of gold nanoparticles from *Scutellaria barbata* and its anticancer activity in pancreatic cancer cell (PANC-1). Artif. Cells Nanomed. Biotechnol. 47(1) 1617-1627,(2019). https://doi.org/10.1080/21691401.2019.1594862.

[66]. Annapoorani A., Koodalingam A., Beulaja M., Saiprasad G., Chitra P, Stephen A., Palanisamy S., Prabhu N. M., You S.G., Janarthanan S., Manikandan R., Eco-friendly synthesis of zinc oxide nanoparticles using *Rivina humilis* leaf extract and their biomedical applications. Process Biochem.112, 192-202(2022). https://doi.org/10.1016/j.procbio.2021.11.022.

Figures

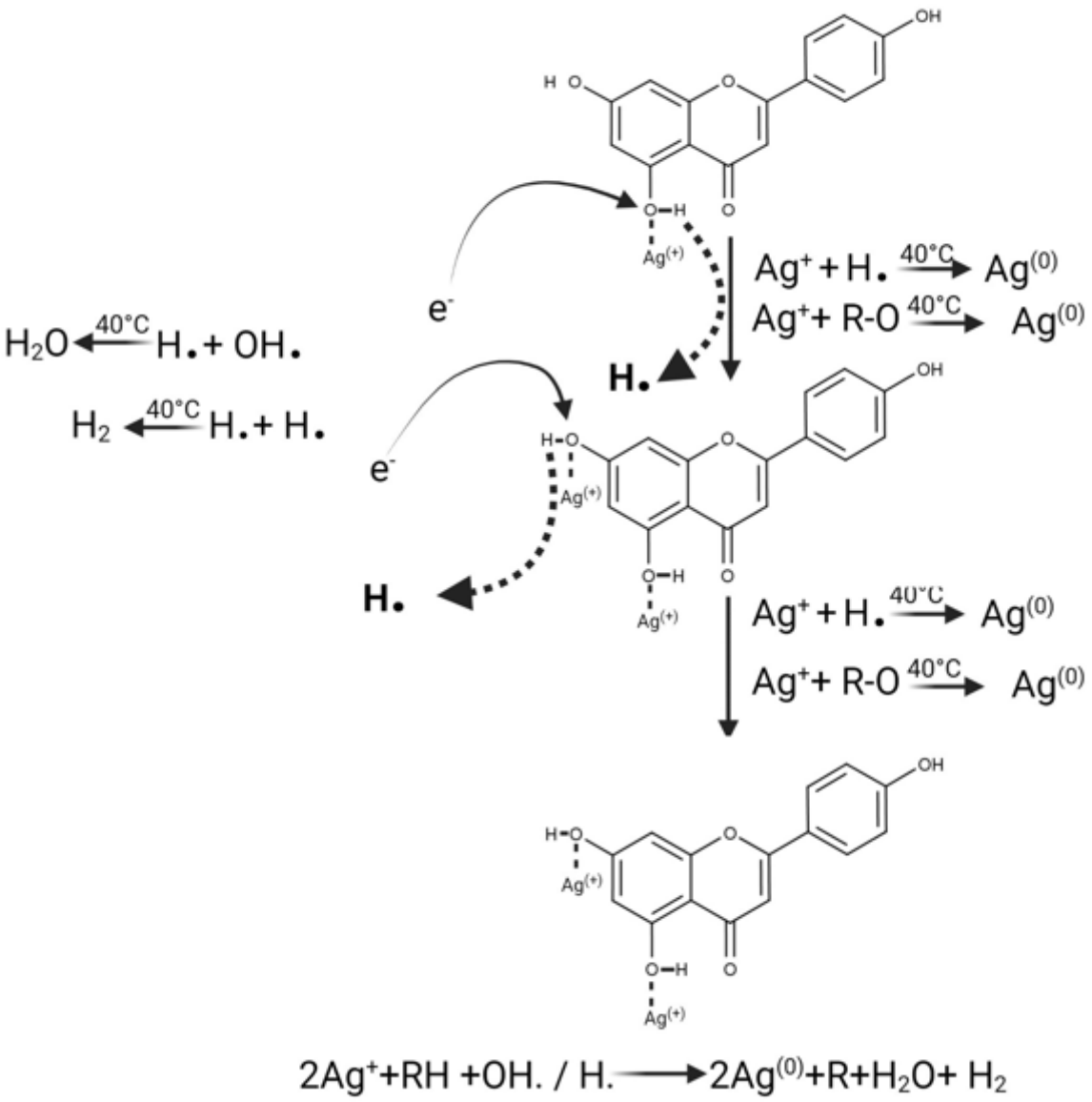

Figure 1

The possible mechanism

The colloidal solution of synthesized PrAgNPs was scanned in the 200-900 nm range using a UV spectrophotometer to determine the formation of PrAgNPs. The specific peak of formed AgNPs was determined at 420 nm.

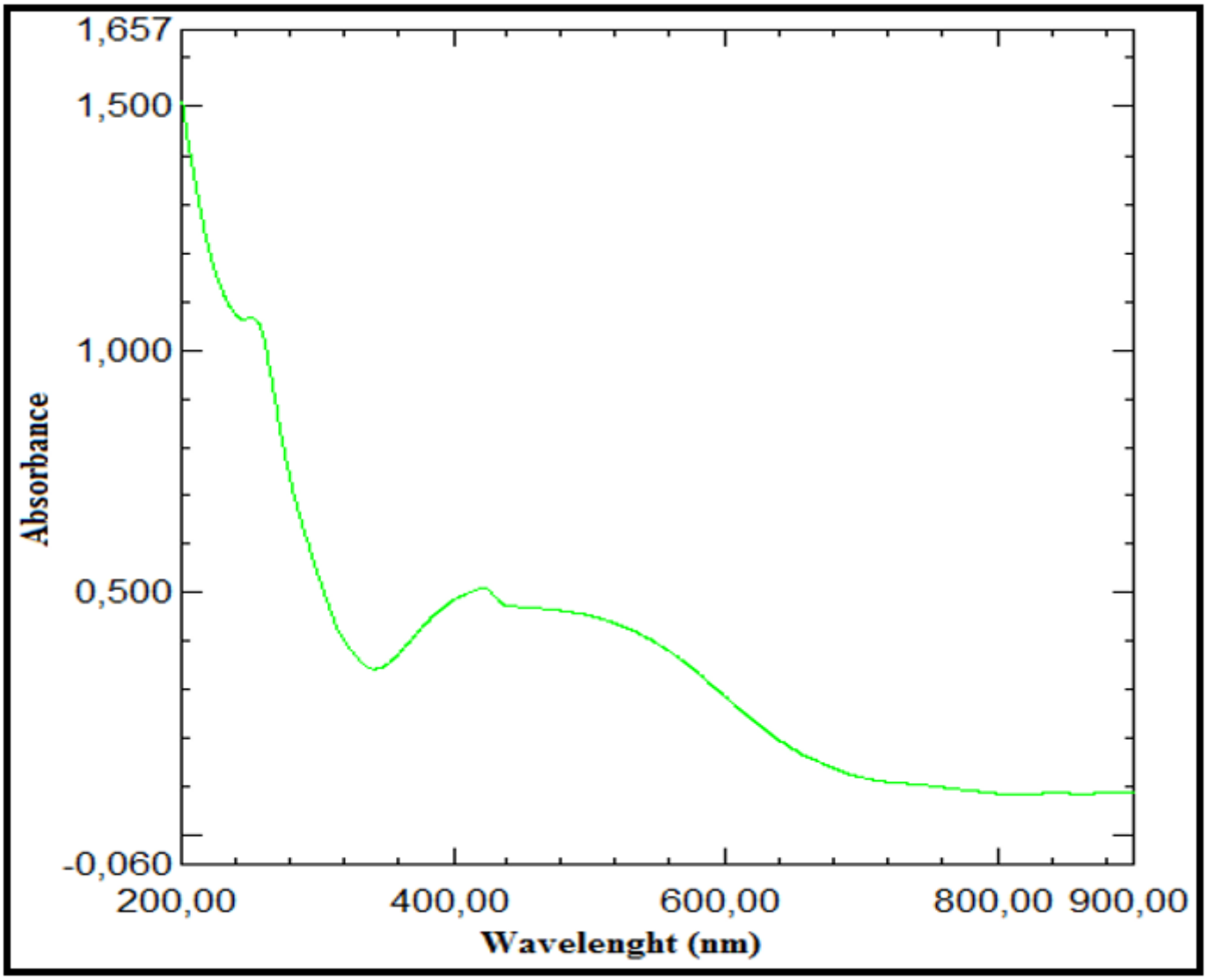

Figure 2

UV-Vis spectra of synthesized PrAgNPs

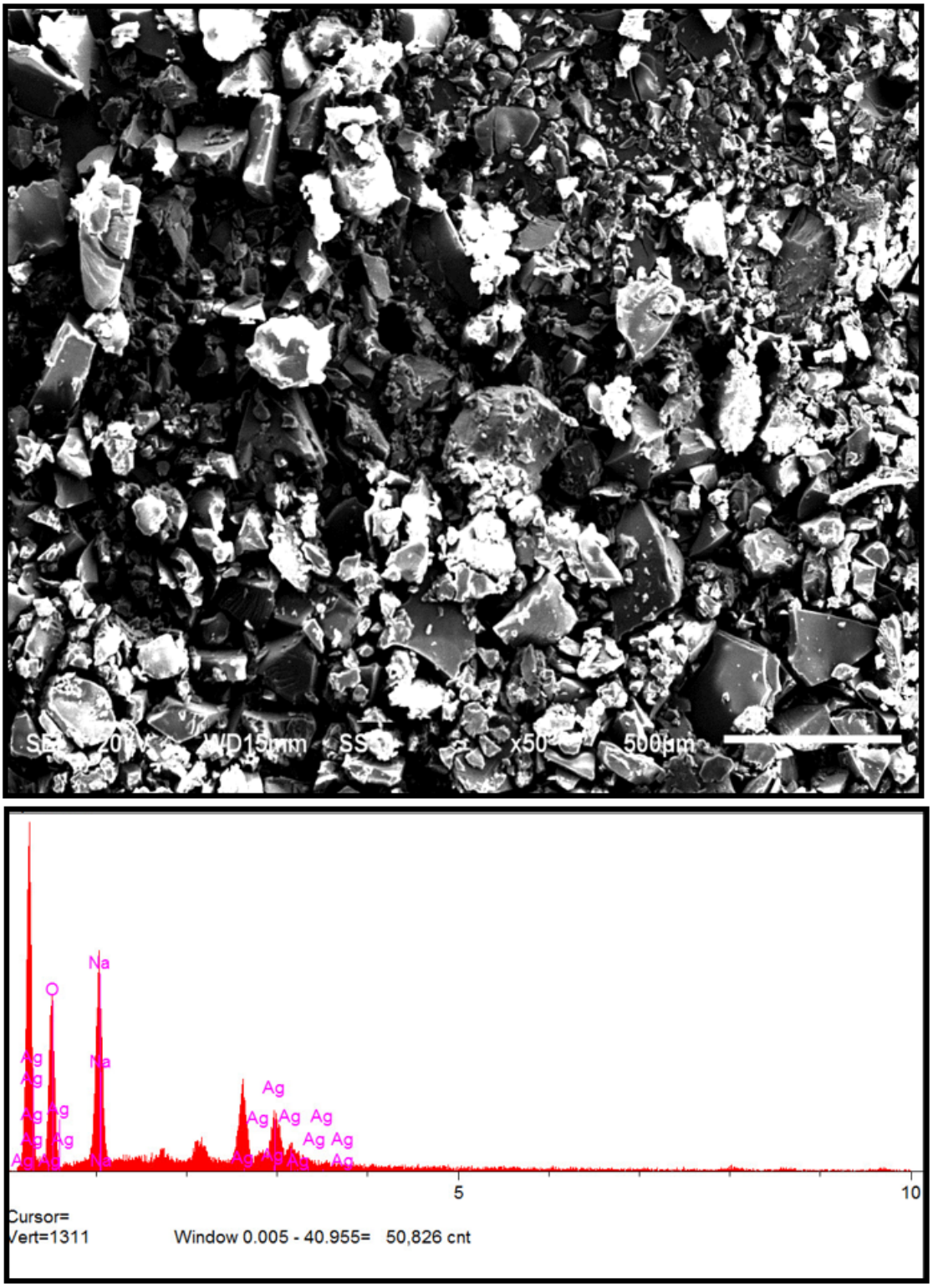

Figure 3

SEM of synthesized PrAgNPs

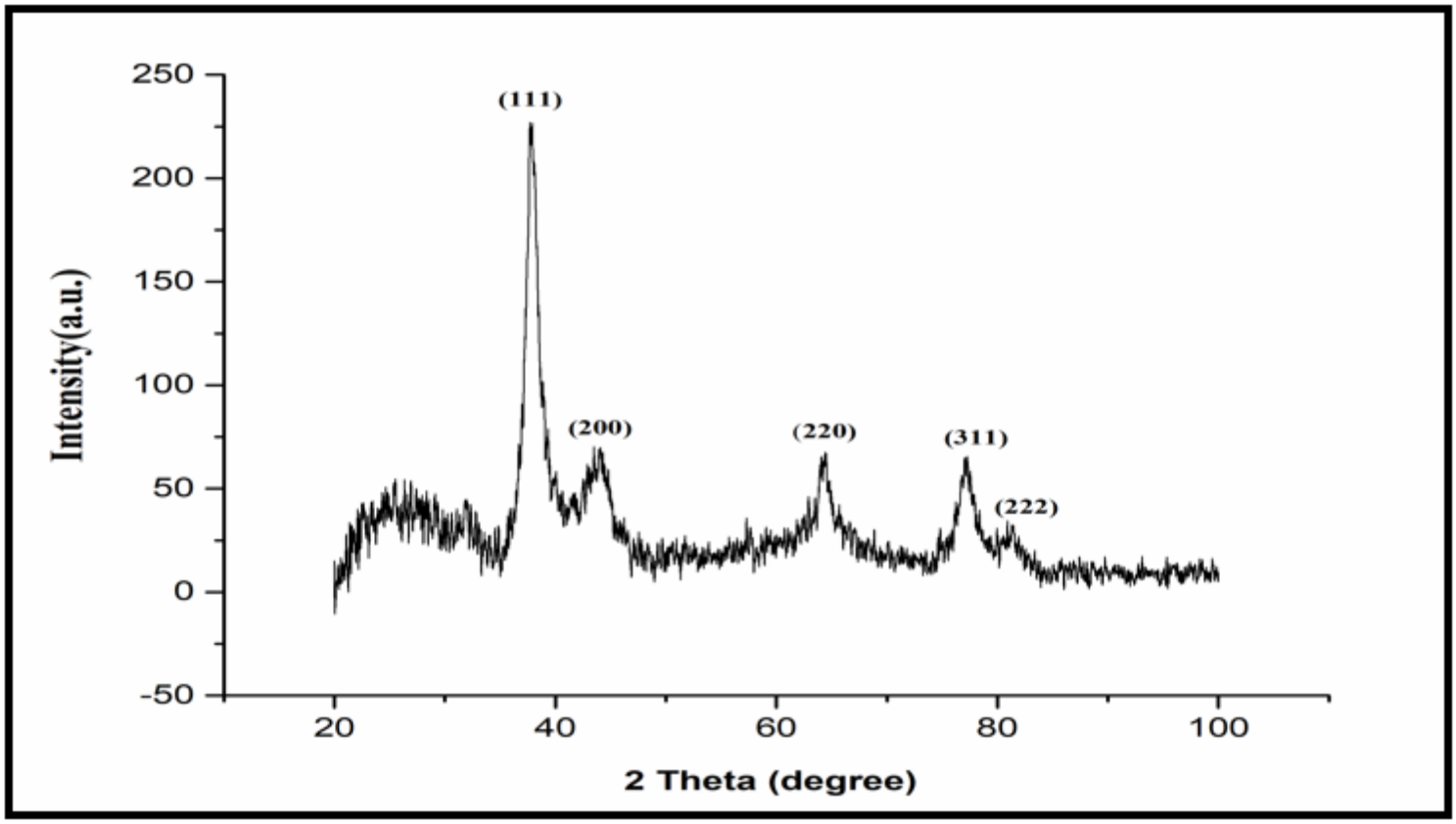

Figure 4

XRD spectra of synthesized PrAgNPs using a Cu source (l 1.5418 Å). Miller indexes for all Bragg reflections are indicated in the figure

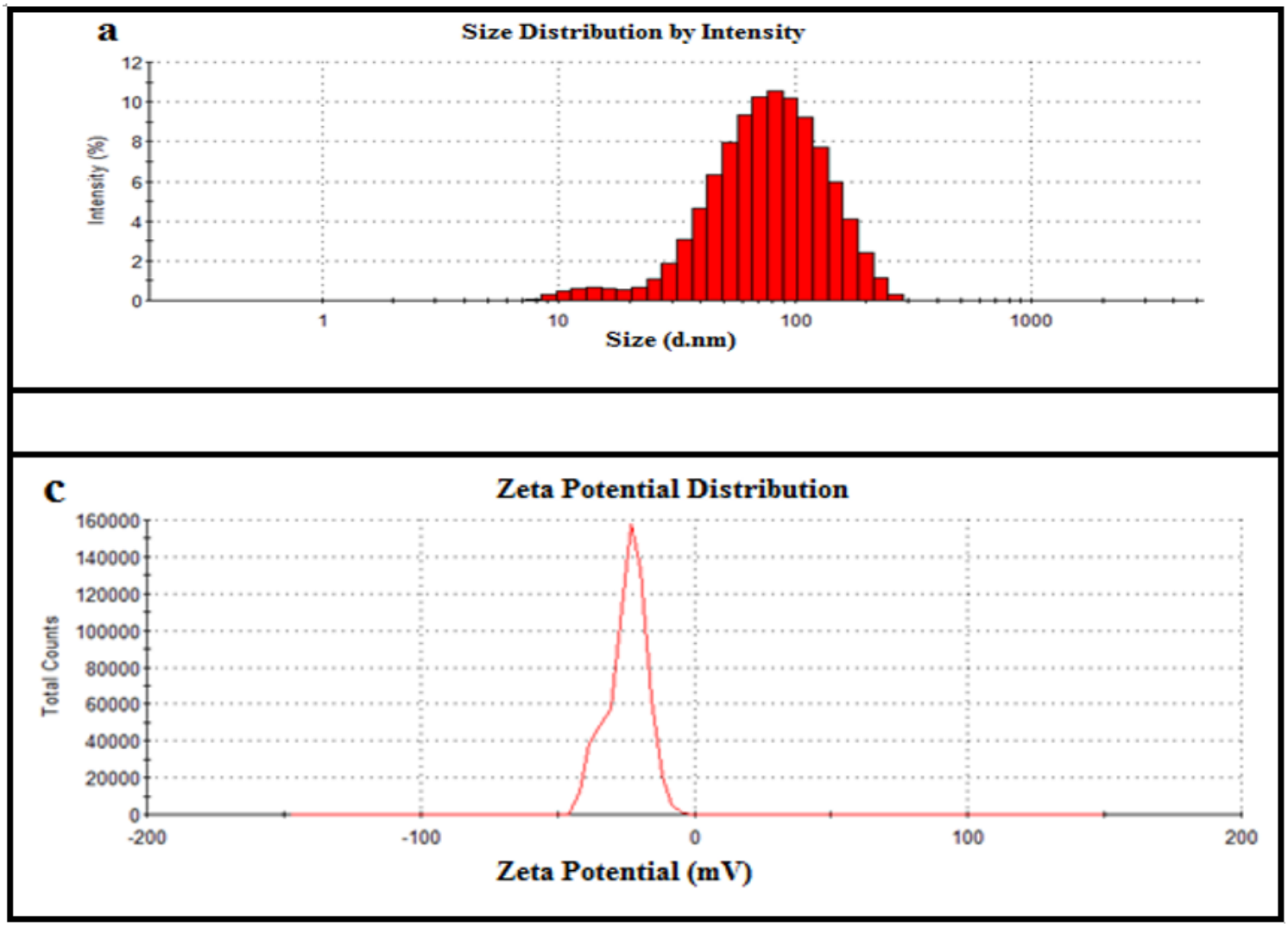

Figure 5

DLS analysis **(a)** and zeta potential **(c)** of PrAgNPs

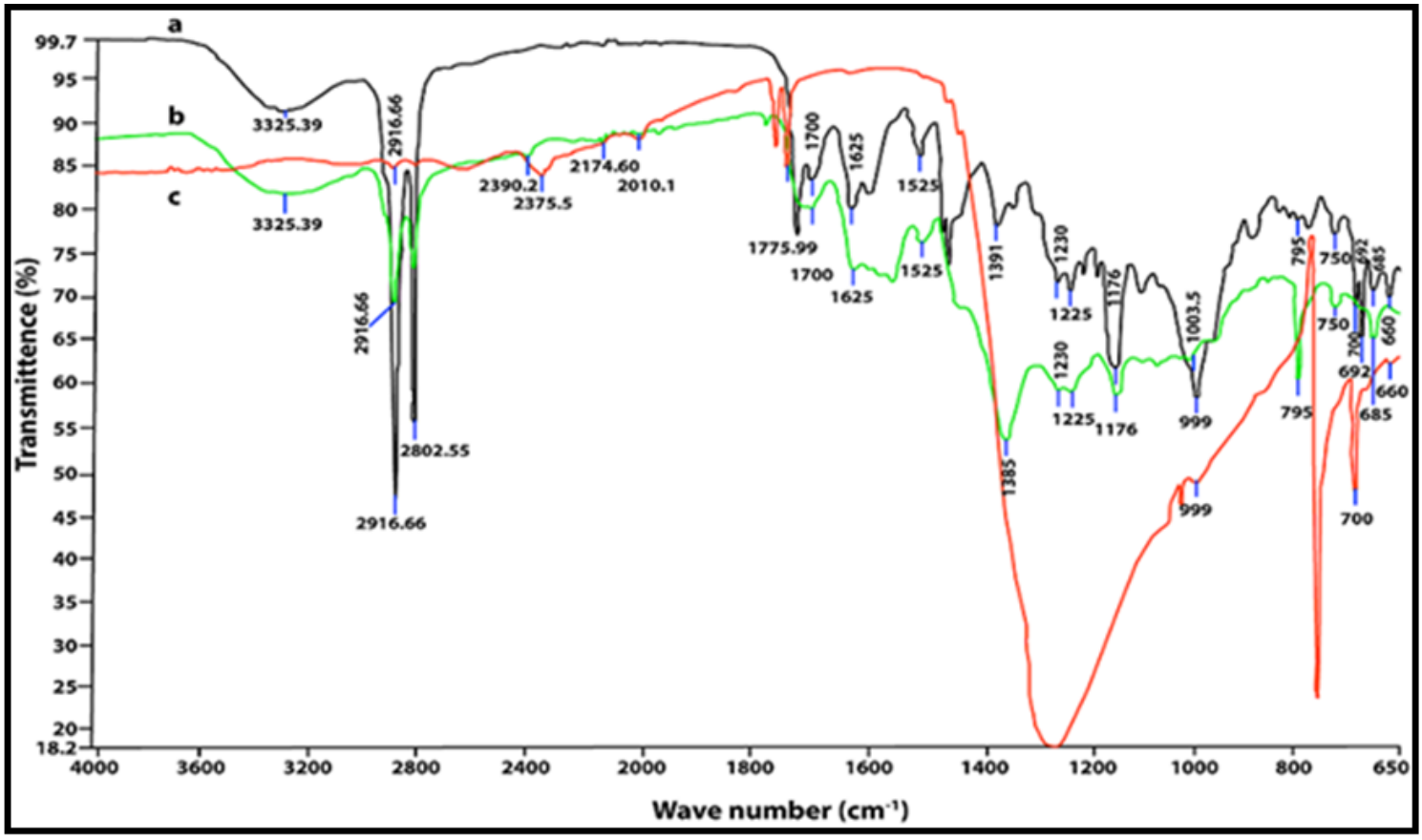

Figure 6

FT-IR spectra of EEP **(a)**, PrAgNPs **(b)**, and $AgNO_3$ **(c)**

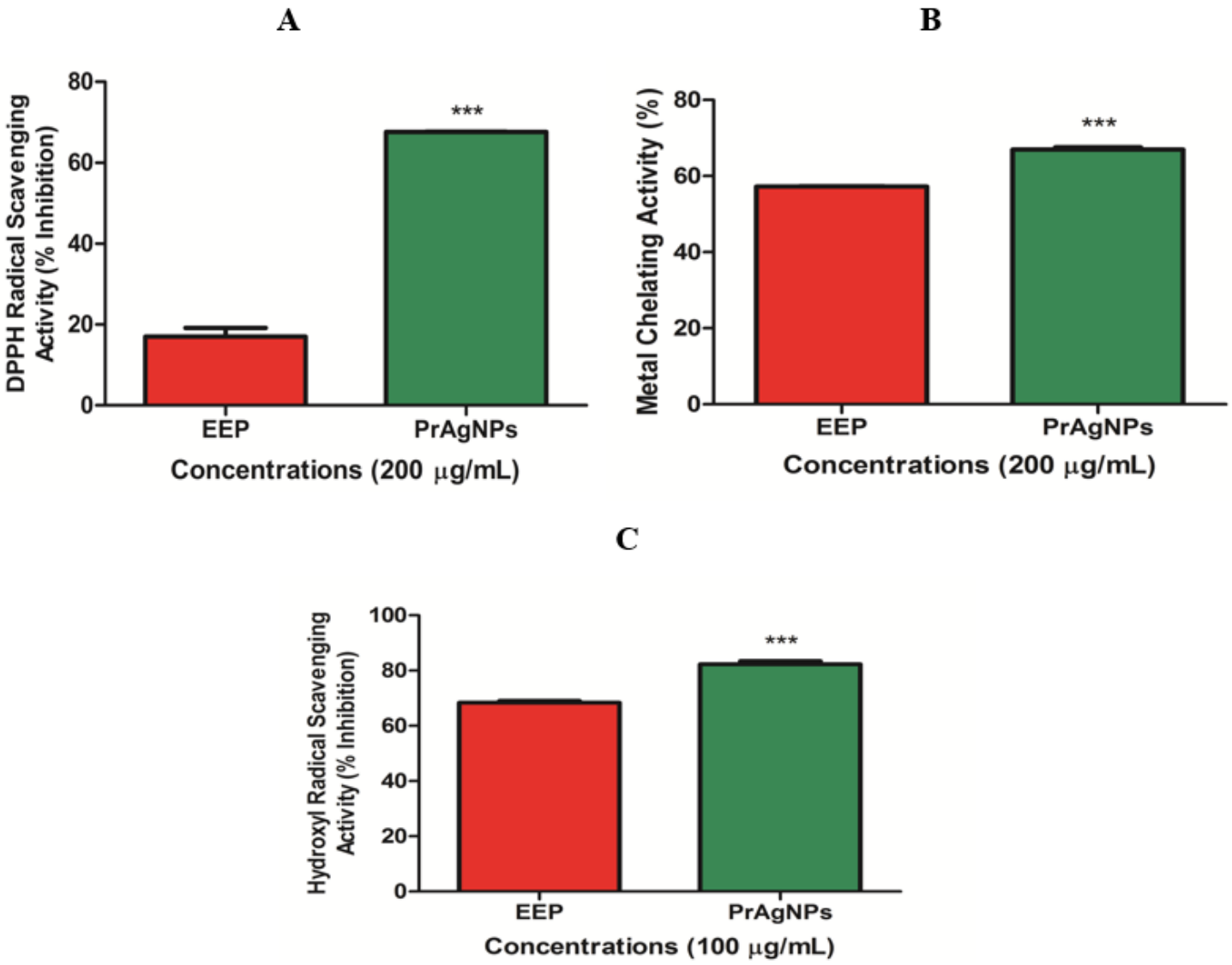

Figure 7

The *in vitro* antioxidant activities of EEP and PrAgNPs. **(A)** Shows the DPPH radical scavenging activity of EEP and PrAgNPs as inhibition rate (%); **(B)** Illustrates the metal chelating activity of EEP and PrAgNPs as chelation rate (%); **(C)** Demonstrates the hydroxyl radical scavenging activity of EEP and PrAgNPs as inhibition rate (%). All data are represented by the mean ± S.D. from 5 independent experiments. *** P <0,001 EEP vs PrAgNPs, as indicated by the brackets.

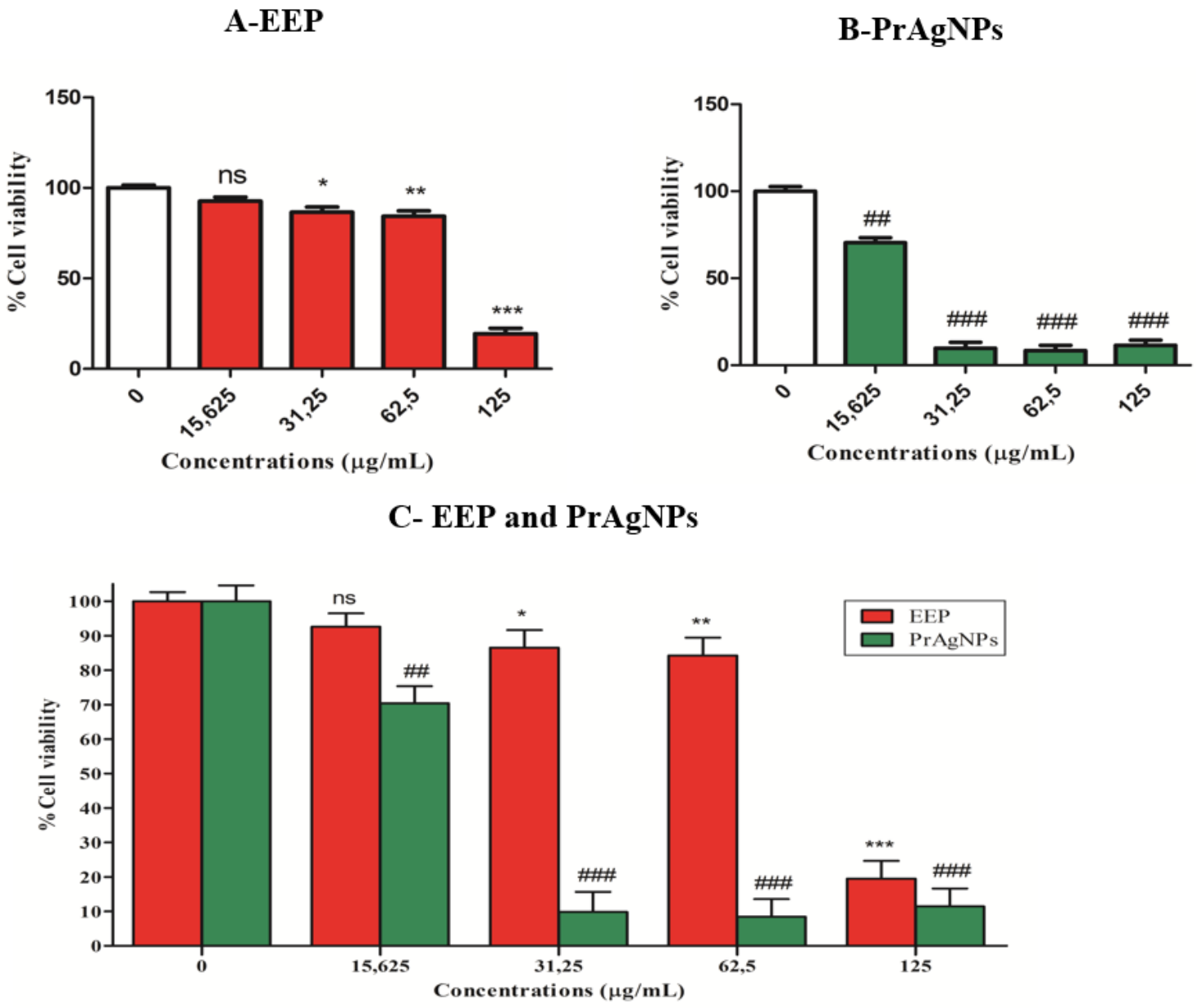

Figure 8

Percent of PC-3 cell viability after treatment with EEP and PrAgNPs. **(A)** Shows the effect of EEP on cell viability in PC-3 cells. The data are represented by the mean ± S.D. from 5 independent experiments. ^{ns} P >0,05, * P <0,05, ** P <0,01, *** P <0,001 vs only EEP control, as indicated by the brackets. (0 µg/mL EEP used as EEP control). **(B)** Illustrate the effects of PrAgNP on cell viability in PC-3 cells. Data are the mean ± S.D. from 5 independent experiments. $^{\#\#}$ P <0,01, $^{\#\#\#}$ P <0,001 vs only PrAgNPs control, as indicated by the brackets. (0 µg/mL PrAgNPs used as PrAgNPs control). **(C)** Shows the effect of EEP and PrAgNPs relative to each other on cell viability in PC-3 cells.

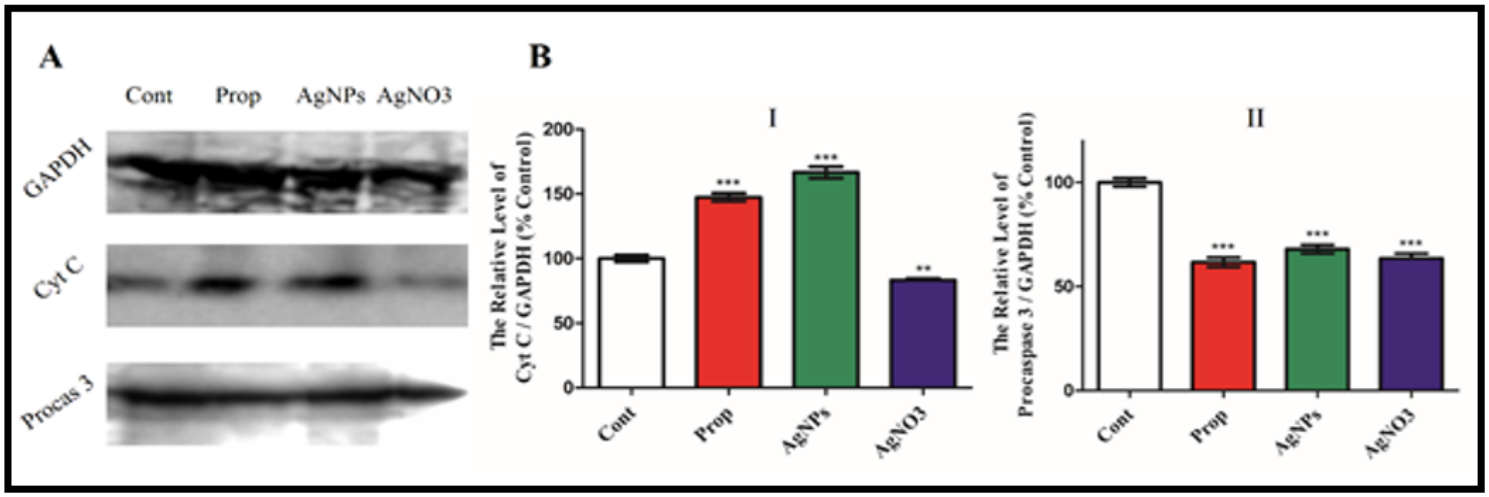

Figure 9

The effects of AgNPs from propolis on apoptosis connected proteins expression in the PC-3 cells. **(A)** The expression of cytochrome *c* (15 kDa) and procaspase-3 (34 kDa) protein levels were measured by Western blot analysis. GAPDH was used as loading control. **(B)** Data are represented by mean ± SEM. (n= 3). *p<0.05 Cont vs Others, **p<0.001 Cont vs Others, ***p<0.001 Cont vs Others. (Cont=Control; Prop=Propolis; AgNPs=AgNPs from propolis; Cyt C= cytochrome *c*; Procas 3= procaspase-3).